DURABILITY AND LIFE PREDICTION OF CHINESE TRADITIONAL BLACK BRICKS UNDER FREEZING AND THAWING CONDITIONS

PENG ZHAO[1] *, QIN LEI[1], XIUZHI ZHANG[2], WENJUAN HUAN[3], HAIJIAN MA[4]
[1]School of Civil Engineering and Architecture, University of Jinan, Jinan Shandong Province, 250022, China.
[2]School of Materials Science And Engineering, University of Jinan, Jinan Shandong Province, 250022, China.
[3]Jiangsu Key Laboratory for Construction Materials, Southeast University, Nanjing Jiangsu Province, 211189, China.
[4]College of Aerospace Engineering, Nanjing University of Aeronautics and Astronautics, Nanjing Jiangsu Province, 211189, China

This experiment takes the mass loss rate and relative dynamic elastic modulus as indicators to study the damage degradation process of black bricks in freezing-thawing environment and sulfate corrosion environment under pressure load, it compares and analyzes the characteristics of freezing-thawing damage and mutual influence of various failure factors. This paper also performs experimental research and theoretical analysis of the process of damage degradation of black bricks under action of freezing-thawing cycles. The study finds that under the action of only freezing-thawing factor, the relative dynamic elastic modulus of the black brick test piece decreases to about 0.60 after 80 cycles of freezing-thawing, reaching the failure criteria of the test piece. The coupling effect of the load and sodium sulfate accelerates the decline of the relative dynamic elastic modulus of the test piece under the action of freezing-thawing. Finally, this paper combines with the freezing-thawing fatigue damage equation model, through the number of indoor freezing-thawing cycles of the black brick, uses the Geographic Information System (GIS) software TopMap7 to draw various freezing-thawing life distribution maps of the black bricks under water freezing, load and salt freezing environment.

Keywords: *Black Brick; Durability; Freezing-Thawing; Life Prediction; Model*

1. Introduction

China has a vast territory and a long history, with an architectural history of more than 7,000 years [1-3]. After thousands of years of struggle, China had various ancient buildings, and diversified architectural remains [4-6]. Ancient Chinese architecture combines science, creativity and artistry, it has a particular style and special functions, and is unique in world architecture. Ancient Chinese architecture is a comprehensive product of political, economic, cultural and technological conditions of specific historical period. Through them, not only can we learn from the treasure house of ancient Chinese architecture, but we can also better understand the history of the Chinese nation, it will have a positive effect on the inheritance of the national culture [7-9].

However, due to the long-term environmental effects such as wind erosion, rain, earthquake and other natural disasters, a large number of ancient buildings face serious damages. For both ancient buildings and pseudo-classic buildings, brick walls are important load-bearing structures or building envelope, and their safety plays a key role in protecting the status of cultural relic architectures [10,11]. At present, the research on the durability mechanism and evaluation of black bricks is scattered and not systematic [12-15]. In addition to the study of durability under the only factor of anti-freezing and anti-sulphate, the research results of the performance of black bricks under the multi-factor coupling of mechanical load and sulfate are few and no public reports have been reported yet.

In this paper, the relative dynamic elastic modulus is used as an indicator to study the damage degradation process of black bricks under the freezing-thawing environment, sulfate corrosion environment and pressure load. The characteristics of freezing-thawing and mutual influence of various damage factors are compared and analyzed. Experimental research and theoretical analysis of the process of damage degradation of black bricks under freezing and thawing cycles are carried out. Referring to the related papers, this paper combines with the freezing-thawing fatigue damage model, targeting on the natural freezing-thawing environment conditions, according to the accumulation principle of fatigue damage, it draws the life prediction distribution map of black bricks under the freezing-thawing conditions throughout China.

2. Materials and Methods

2.1. Experimental materials

The experiment selected black bricks produced by Changzhou Longyun Antique Building Materials Co., Ltd., the chemical composition is shown in Table 1. Ten black bricks were taken for physical property test, the average values are shown in

* Autor corespondent/*Corresponding author*,
E-mail: zhaopeng_610@163.com

Table 1

Chemical composition of black brick wt%

Type	SiO_2	Al_2O_3	FeO	MgO	CaO	TiO_2	K_2O	Na_2O
Black brick	69.45	14.13	9.18	1.93	0.47	0.65	4.51	0.47

Table 2

Physical and mechanical properties of black brick

Data type	Size/mm	Density/(kg/m^3)	Compressive strength /MPa	Water absorption rate /%
Average value	230×115×48	1828	8.11	12.45

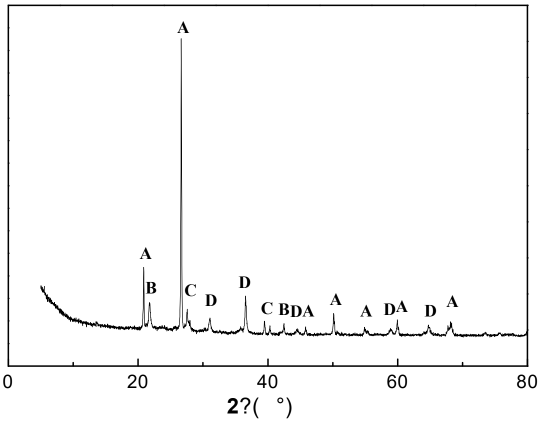

Fig.1 - XRD pattern of black brick

Table 2. The mineral composition is shown in Fig. 1. The mineral composition of the black bricks mainly includes quartz (A), albite (B), anorthite (C), and hercynite spinel (D).

2.2. Experimental Method

In order to simulate the durability behavior of black bricks in the natural environment, the freezing-thawing cycles, sodium sulfate corrosion and external compressive stress are selected to carry out the durability test of black bricks under single, double and multiple factors. There are 3 major categories of experiments. Three bricks were selected for each test.

(1) Durability of black bricks under the action of the single freezing-thawing factor.

(2) Durability of black bricks under the action of double factors, including freezing-thawing + 10% load, freezing-thawing +30% load.

(3) Durability of black bricks under triple factors, including freezing-thawing + 10% load + 5% sulfate solution, freezing-thawing + 30% load + 5% sulfate solution.

2.2.1. Single failure factor

According to GB/T 2542-2012, after the test piece had been immersed for 24 h, it was placed in a freezing-thawing box(JY-BX-115) at -15 °C~-20 °C for 3 h, then it was taken out and placed in 15 °C~20 °C water for 3 h, every six hours is a cycle. During the experiment, the sample was immersed in water for 24 h, and the surface water was wiped dry to measure the initial ultrasonic sound time interval T_0 using the ultrasonic instrument, for every 5-10 cycles, measures the ultrasonic sound time interval T_n, the relative dynamic elastic modulus Er was calculated by formulas (1):

$$E_r = \frac{E_n}{E_0} = \frac{V_n^2}{V_0^2} = (\frac{T_0}{T_n})^2 \tag{1}$$

2.2.2. Multiple failure factors

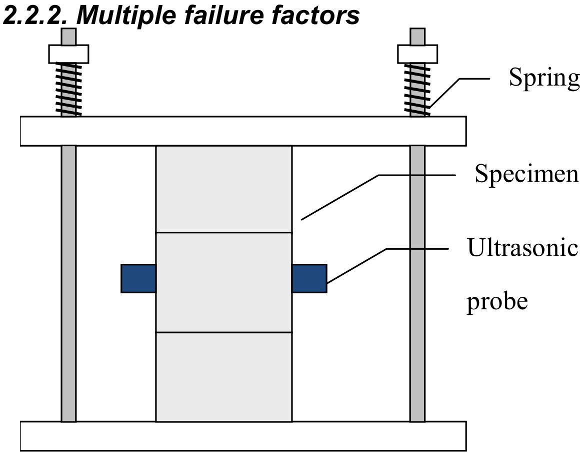

Fig. 2 - Device diagram of test piece subjected to compressive stress

At the same time as the freezing-thawing cycle experiment, compressive stress was applied to the sample as shown in Fig. 2. The device is cleverly designed and easy to use, it improves the utilization rate of the freezing-thawing test machine. First measure the elastic modulus of the spring, and then control the load by the amount of compression of the spring. The tests have shown that with this loading device, the thermal expansion of the test piece and the instrument, as well as the temperature change of the freezing-thawing cycle, have little effect on the load of the test piece.

A spring-loading system was used to apply compressive stress to the black brick test piece, which is equivalent to 10% and 30% of its compressive damage strength, and then the freezing-thawing cycle compressive stress experiment was started. The test piece was placed in a freezing-thawing test machine together with the loading device, and the freezing-thawing test was carried out according to GB/T 2542-2012. In the third category experiment, the specimens were melted in 5% sulphate solution for three hours during each freeze-thaw cycle.

3. Experimental results and discussion

3.1. Single freezing-thawing factor

It can be seen from Fig. 3 that as the number of freezing-thawing cycles increases, the relative dynamic elastic modulus of the three black bricks slightly increases at first and then decreases. Before 35 freezing-thawing cycles, the relative dynamic elastic modulus of the bricks increased and fluctuated between 1-1.15; after 35 cycles, the relative dynamic elastic modulus decreased slowly, and the relative dynamic elastic modulus of the three brick samples decreased to about 0.60 after 80 freezing-thawing cycles. With the rise in freeze-thaw cycle frequency, the brick will see increasing internal microcrack and gradual decline in relative dynamic modulus of elasticity. At the time when obvious exfoliation takes place on the brick surface, it's impossible to detect the ultrasonic velocity with ultrasonoscope due to unsmooth exfoliation on brick corners.

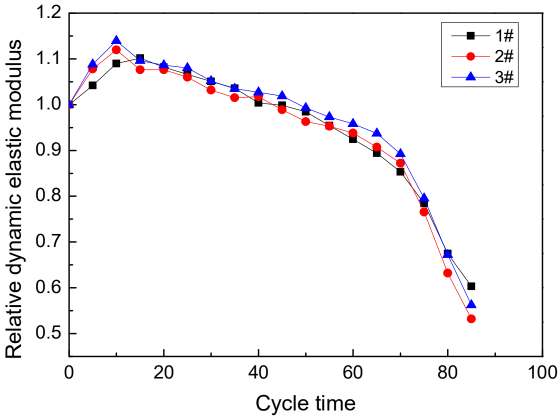

Fig.3 - Relative dynamic modulus of black bricks subjected to freezing-thawing cycles

3.2. Effect of load on the freezing resistance of black bricks

Fig. 4 and 5 show the effect of load on the freezing resistance of black bricks. The results show that the load effect has obvious influence on the relative dynamic elastic modulus, and the load action accelerates the decline rate of the relative dynamic elastic modulus of the test piece under the action of freezing and thawing. It can be seen from the figure that after applying 10% load, as the number of freezing-thawing cycles increases, the relative dynamic elastic modulus of the three black bricks slightly increases at first and then decreases. After about 50 freezing-thawing cycles, the relative dynamic elastic modulus of the black brick samples began to show a significant declining trend. After 60 freezing-thawing cycles, the relative dynamic elastic modulus decreased to below 60%, which reaches the failure criteria of the test piece. After applying 30% load, the relative dynamic elastic modulus of the black brick samples showed a significant declining trend after about 30 freezing-thawing cycles. After 35 freezing-thawing cycles, the relative dynamic elastic modulus decreased to below 60%, which reaches the failure criteria of the test piece. Under the joint effects of load and freeze-thaw, the brick body destruction goes in the same way as in conditions affected by single freeze-thaw factors - the surface peels off as a result of crack extension. Due to the load effect, however, the destruction goes a little faster.

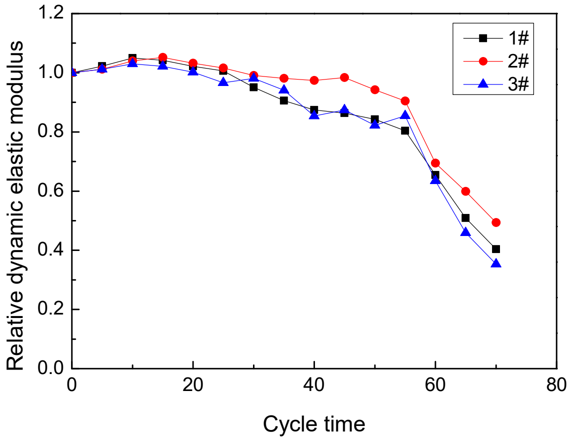

Fig.4 - Relative dynamic elastic modulus of black bricks subjected to freezing-thawing cycles and 10% load

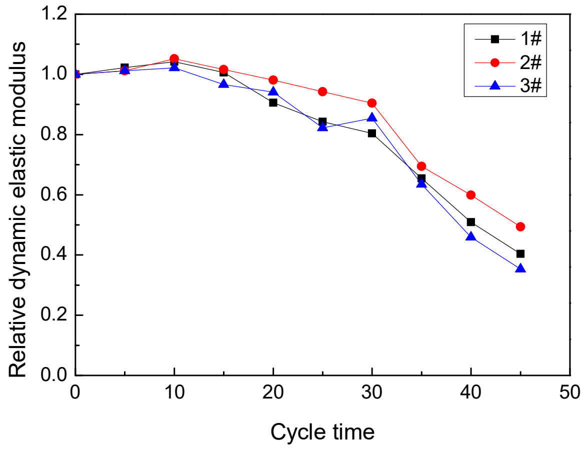

Fig.5 - Relative dynamic elastic modulus of black bricks subjected to freezing-thawing cycles and 30% load

3.3 Effect of load and crystallization of sodium sulfate (Na_2SO_4) on the freezing resistance of black bricks

Figures 6 and 7 show the effect of load and sodium sulfate crystallization on the freezing resistance of black bricks. The results show that the brick surface saline solution gets increasingly high in concentration; where the concentration exceeds the solubility concentration, salt will be precipitated in the form of crystals. When crystalized, salt will experience a volume expansion; once the crystal swelling stress exceeds the tensile force that the surface pore wall can bear, the piezocrystallization will cause repeated destruction to the brick body.. The coupling of load and sodium sulfate accelerates the declining rate of the relative dynamic elastic modulus of the test piece under the action of freezing and thawing. It can be seen from the figure that under the action of 10% load and 5% sodium sulfate solution, the relative dynamic elastic modulus of the three black bricks slightly increases first and then decreases with the increase of the number of freezing-thawing cycles. After about 25 freezing-thawing cycles, the relative dynamic elastic modulus of the black brick samples began to show a significant declining trend. After 35 freezing-thawing cycles, the relative dynamic elastic modulus decreased to less than 60%, reaching the failure criteria of the test piece. Under the action of 30% load and 5% sodium sulfate solution, the relative dynamic elastic modulus of the black brick samples showed a significant declining trend after about 10 freezing-thawing cycles, and the relativedynamic elastic modulus decreased to below 60% after 20 freezing-thawing cycles, which reaches the failure criteria of the test piece.

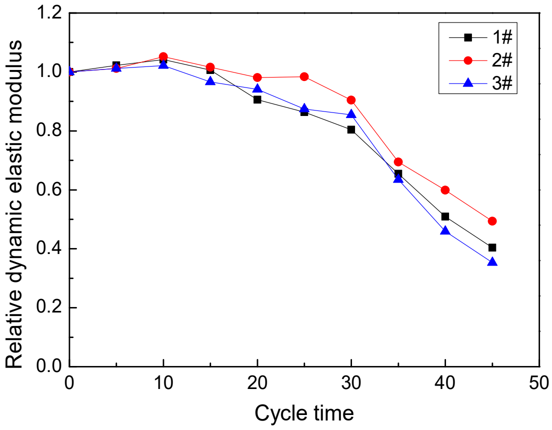

Fig.6 - Relative dynamic elastic modulus of black bricks subjected to freezing-thawing cycles and 10% load and 5 wt% sodium sulfate

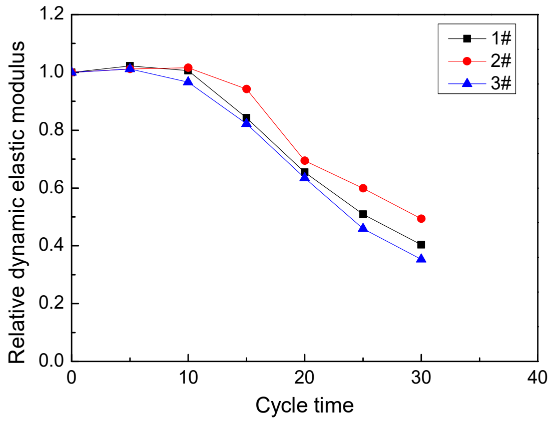

Fig.7 - Relative dynamic elastic modulus of black bricks subjected to freezing-thawing cycles and 30% load and 5 wt% sodium sulfate

4. Fatigue damage model of freezing-thawing of black bricks and prediction method of freezing-thawing life

The fatigue of the black bricks is a process in which the material properties gradually change, which in turn causes the cracking and expansion of the micro-cracks of the black brick until the main crack is formed. This process is accompanied by changes in strain and ultrasonic velocity, i.e. the fatigue damage. Fatigue strength is the level of alternating fatigue stress for a given number of cycles when the corresponding standard test piece is subjected to fatigue failure, normally it is expressed as a fraction of its static strength. The relationship between the number N of any specified cycles and the corresponding fatigue strength S can be expressed by a stress-fatigue life curve, and an S-N curve or a Wohler curve.

The macroscopic characteristics of the black bricks gradually decrease during thethawing cycles, which is mainly reflected in the decrease in compactness and the decrease in strength [16-19]. Scanning electron microscopy and X-ray diffraction analysis show that the freezing-thawing damage of the black bricks is actually a process from dense to loose, which is accompanied by the appearance and development of micro-cracks. Although hydrostatic pressure is a uniform internal pressure, and unidirectional tension is an external tensile force, and the action modes of the two forces are different, while the black brick is a non-uniform brittle material, under the action of three-direction uniform tensile stress, it's always the weakest section that is destroyed first, therefore, the action of the freezing-thawing cycle and the triaxial tension are similar in the damage of the black bricks. The triaxial tension can be used to simulate the internal tensile stress during the freezing and thawing process of the black bricks. On this basis, Yu Hongfa's research group proposed a freezing-thawing fatigue damage life prediction model [20], as follows:

4.1. Freezing-thawing fatigue damage model

Tepfers [21] gives the following expressions for the fatigue strength of the test piece under uniaxial tensile stress, which can also be used for that under the triaxial tensile stress:

$$S = \frac{\sigma_{\max}}{f_t} = 1 - \beta(1-R)\lg N \quad (3)$$

Where, σ_{max} and σ_{min} are the maximum and minimum tensile stress (MPa), respectively;

f_t—Tensile strength (MPa);

β—Material parameter;

R—Stress ratio ($\sigma_{min}/\sigma_{max}$);

N—Fatigue life (times).

According to the definition of damage mechanics, the damage variable D_n represents the loss rate of the dynamic elastic modulus after n freezing-thawing cycles of the test piece [22].

$$D_n = 1 - \frac{E_n}{E_0} \quad (4)$$

Where, E_0 and En respectively are the dynamic elastic modulus of the test piece before the freezing-thawing cycles and after N cycles of freezing-thawing.

For the initial state, the freezing-thawing damage D_0=0, and the stress-strain constitutive relationship of the damaged test piece is considered as follows:

$$f_{tn} = E_n \cdot \varepsilon_t = E_0 \cdot (1 - D_n) \cdot \varepsilon_t = f_{t0} \cdot (1 - D_n) \quad (5)$$

f_{t0} and f_{tn} are the tensile strength of the test piece before the freezing-thawing cycles and after n cycles of freezing-thawing, εt is the ultimate tensile strain of the test piece.

In addition, in the freezing-thawing cycle process, the maximum internal tensile stress of the test piece occurs during the expansion of the ice, and the minimum tensile stress occurs after dissolution. It can be seen that the freezing-thawing cycle of the test piece is actually equivalent to a tensile fatigue loading process. For the convenience of model simplification, the minimum tensile stress at this time is assumed as σ_{min}=0. Therefore, the stress ratio R=0[19], then the formula (3) is simplified as:

$$S_0 = \frac{\sigma_{\max}}{f_{t0}} = 1 - \beta \lg N \quad (6)$$

In the formula, the fatigue life N is the freezing-thawing fatigue life of the test piece.

After the test piece has undergone n freezing-thawing cycles, the remaining freezing-thawing fatigue life is (N-n), which has the following relationship:

$$S_n = \frac{\sigma_{\max}}{f_{tn}} = 1 - \beta \lg(N - n) \quad (7)$$

From formula (6) and (7), we can get:

$$\frac{f_{tn}}{f_{t0}} = \frac{f_{t0} \cdot (1 - D_n)}{f_{t0}} = \frac{1 - \beta \lg N}{1 - \beta \lg(N - n)} \quad (8)$$

Therefore, the freezing-thawing fatigue damage equation of the test piece is:

$$D_n = 1 - \frac{1 - \beta \lg N}{1 - \beta \lg(N - n)} \qquad (0 \le n \le N - 1) \quad (9)$$

4.2. Material parameter β

It can be seen from the freezing-thawing fatigue damage equation that the size of the freezing-thawing fatigue damage is closely related to the material parameter *β*. For the same stress level S, the larger the material parameter *β*, the smaller the freezing-thawing fatigue life, and the material parameter *β* is an important indicator that measures the freezing resistance of the test piece. In the same freezing-thawing environment, the smaller the material parameter *β*, the better the freezing resistance of the test piece. According to the experimental results of indoor freezing and thawing, when n=N-1, the material parameter *β* value of different test pieces can be obtained from formula (10).

$$\beta = \frac{D_{N-1}}{\lg N} \quad (10)$$

4.3 Freezing-thawing life prediction model of concrete structures under natural freezing and thawing conditions

Assuming that there are m freezing-thawing cycles in a certain winter, the maximum tensile stress $\sigma_{i,max}$ of the test piece undergoing freezing-thawing cycles can be obtained by the condition of every positive and negative temperature change, and then by formula (6) we can get the freezing-thawing fatigue life N_i of the test piece under the action of $\sigma_{i,max}$.

$$\frac{\sigma_{i,\max}}{f_{t0}} = 1 - \beta \lg N_i \quad (11)$$

Comparing formula (6) with (11), the ratio of maximum tensile stress under indoor freezing-thawing condition and natural freezing-thawing condition is obtained as:

$$k = \frac{\sigma_{\max}}{\sigma_{i,\max}} = \frac{1 - \beta \lg N}{1 - \beta \lg N_i} \quad (12)$$

After finishing, the freezing-thawing fatigue life of the test piece under natural freezing-thawing damage according to a specific freezing-thawing cycle system is obtained as:

$$N_i = 10^{\frac{k + \beta \lg N - 1}{\beta k}} \quad (13)$$

Where, σ_{max} is the maximum tensile stress (MPa) during standard indoor rapid freezing and thawing;

$\sigma_{i,max}$ is the maximum tensile stress (MPa) of the test piece when freezing and thawing under a specific freezing-thawing cycle system;

k—Stress ratio ($\sigma_{max}/\sigma_{i,max}$)

N is indoor rapid freezing-thawing fatigue life (times);

N_i is the freezing-thawing fatigue life (times) of test piece under natural condition according to a specific freezing-thawing cycle system.

According to the fatigue damage accumulation principle of the test piece, under the condition of natural freezing-thawing cycle, the freezing-thawing damage caused by the failure of the test piece is caused by the accumulation of freezing-thawing damage generated each time under the specific freezing-thawing cycle system. Therefore, for the freezing-thawing life prediction model of the test piece, the number of years N_{year} that it can withstand the freezing and thawing damage caused by natural winter (consisting of m different freezing-thawing cycles) is:

$$N_{year}=\frac{1}{\sum_{i=1}^{m}\frac{1}{N_i}}=\frac{1}{\sum_{i=1}^{m}\frac{1}{10^{\frac{k+\beta\lg N-1}{\beta k}}}} \qquad (14)$$

Where: N_{year} is the freezing-thawing life (years) of the test piece under natural freezing and thawing conditions.

β—Material parameter($\beta=\frac{D_{N_{indoor}-1}}{\lg N_{indoor}}=\frac{0.4}{\lg N_{indoor}}$)

The stress ratio k in the freezing-thawing life prediction model of the test piece is organically associated with the lowest temperature in the indoor and outdoor environment and the maximum indoor and outdoor temperature drop rate, so that the number of freezing-thawing damages in the natural environment and the number of indoor standard experimental freezing-thawing cycles can be converted.

$$\kappa=\frac{\sigma_{\max}}{\sigma_{i,\max}}=\frac{\left(T\ln\frac{p_w}{p_i}\right)_{indoor}}{\left(T\ln\frac{p_w}{p_i}\right)_{outdoor}}=\frac{\left(\frac{d\theta}{dt}\right)_{indoor}}{\left(\frac{d\theta}{dt}\right)_{outdoor}} \qquad (15)$$

Where: T is indoor or outdoor lowest thermodynamic temperature (t+273.15);

$\frac{d\theta}{dt}$ is indoor or outdoor maximum temperature droprate (℃/min);

$\ln\frac{p_w}{p_i}$ is a semi-empirical relationship equation when the freezing point of ice and the relative steam pressure reach balance.

4.4 Black brick freezing-thawing life distribution maps

The internal factors affecting the durability of black bricks can be obtained through a large number of experimental studies. The acquisition of external factor data affecting the durability of black bricks needs to be obtained from other industries by means of survey statistics, environmental meteorological data is used as a basic scientific data resource. China's meteorological department has long established a comprehensive meteorological monitoring, data collection and data statistics system, and preserves relatively complete meteorological science data of China. To meet the needs of architecture and transportation planning and design, China has established an observingsystem with more intensive weather stations and more detailed monitoring data since 1980. The raw meteorological data affecting the durability of black bricks collected in this paper comes from the National Meteorological Information Center of China Meteorological Administration, and we need to reorganize, count and analyze the original data. Starting from the durability distribution of black bricks in the cold area, we selected 520 meteorological stations taking the Yangtze River basin as the bound,

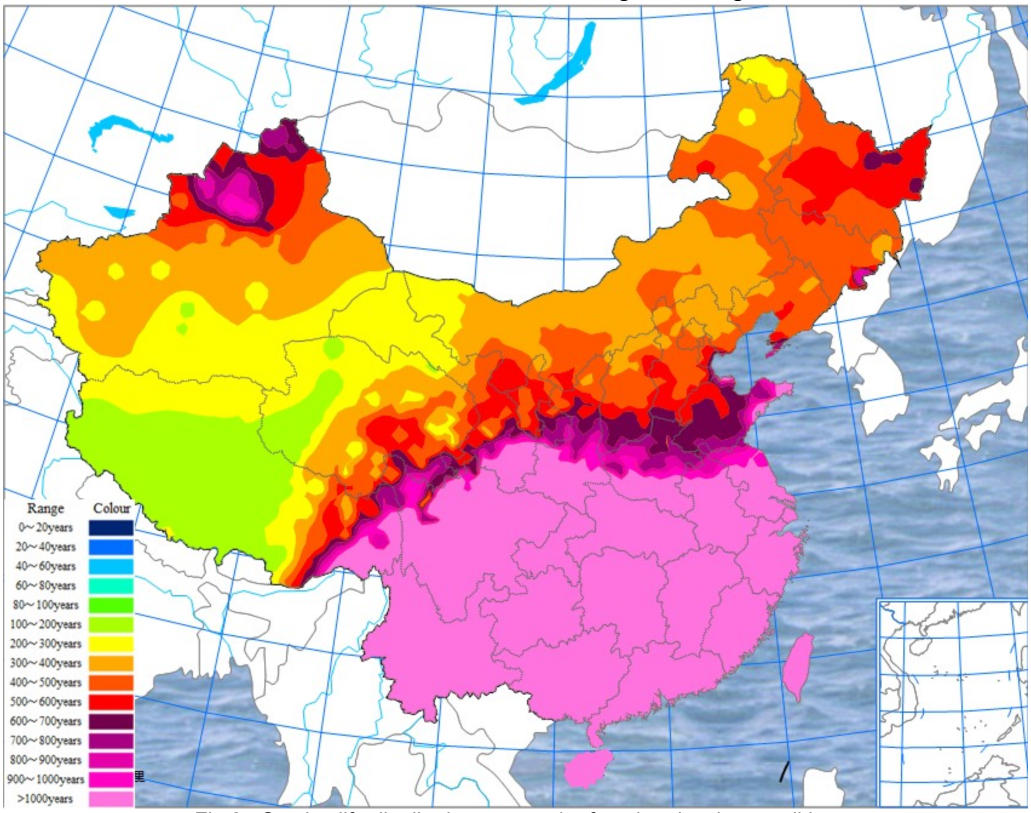

Fig.8 - Service life distribution map under freezing-thawing condition

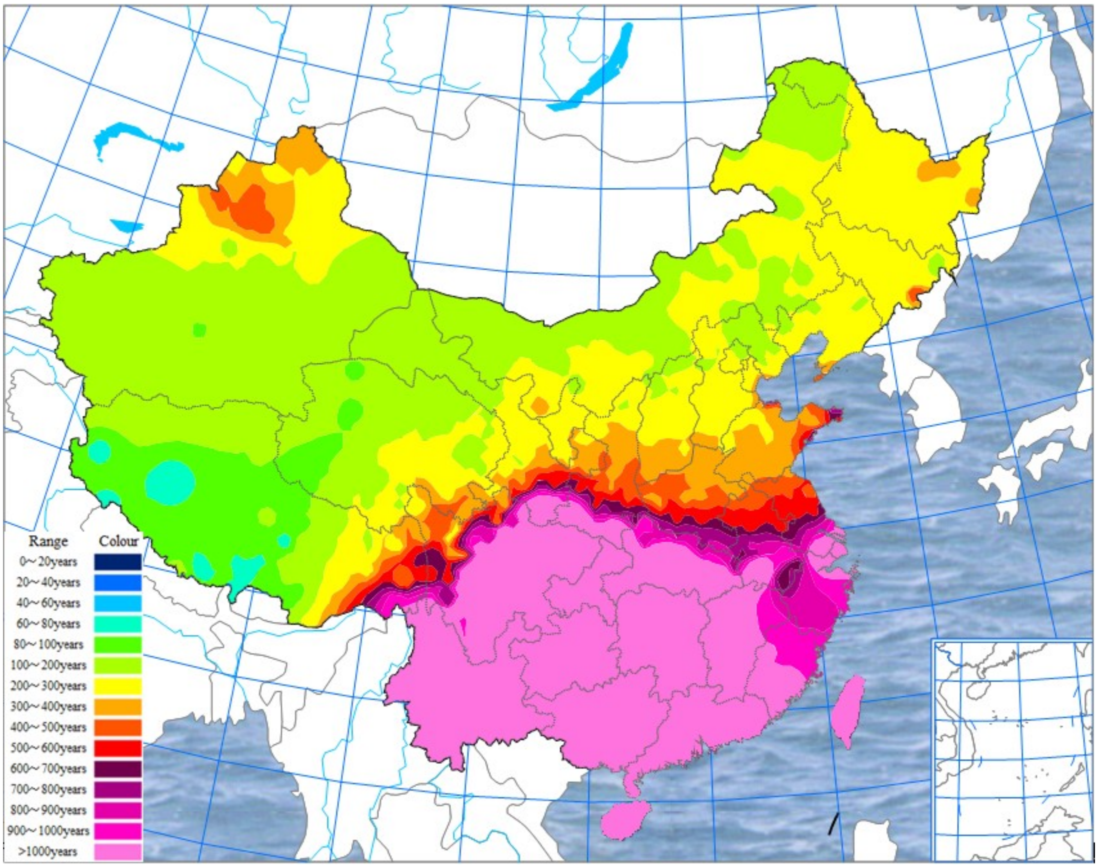

Fig.9 - Service life distribution map under freezing-thawing +10% load

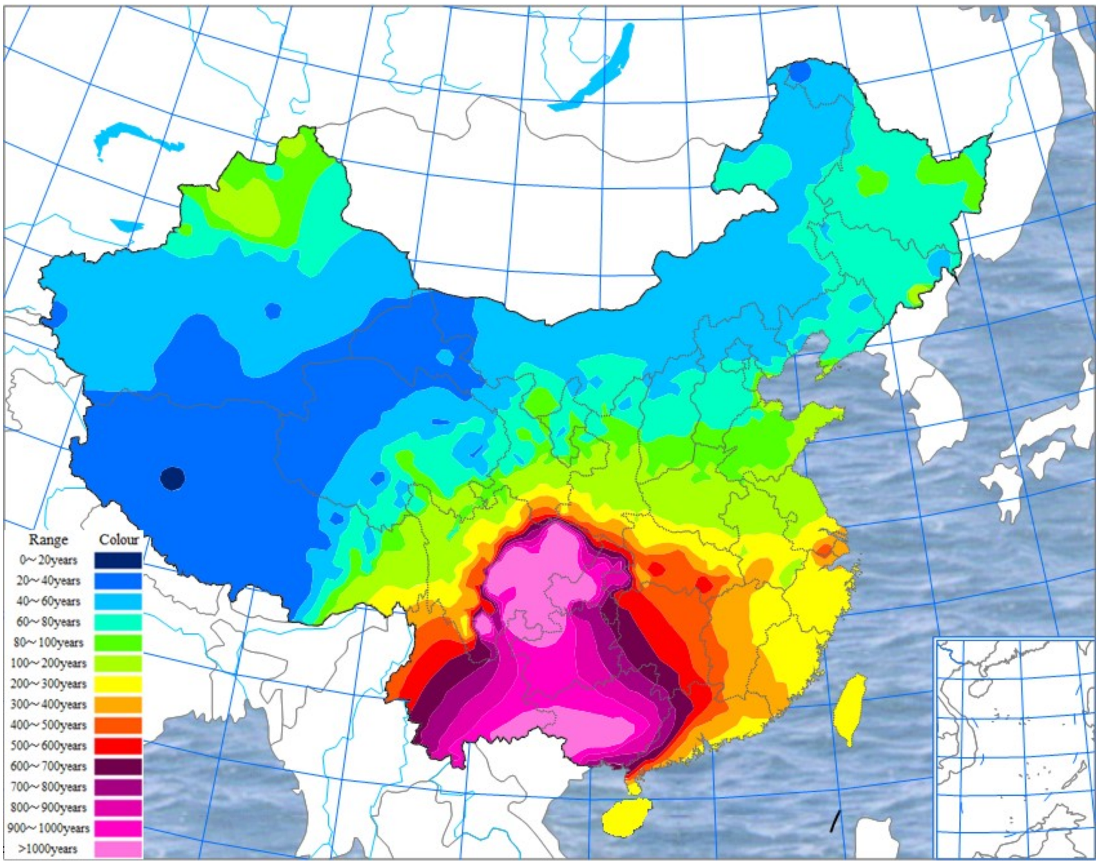

Fig.10 - Service life distribution map under freezing-thawing +30% load

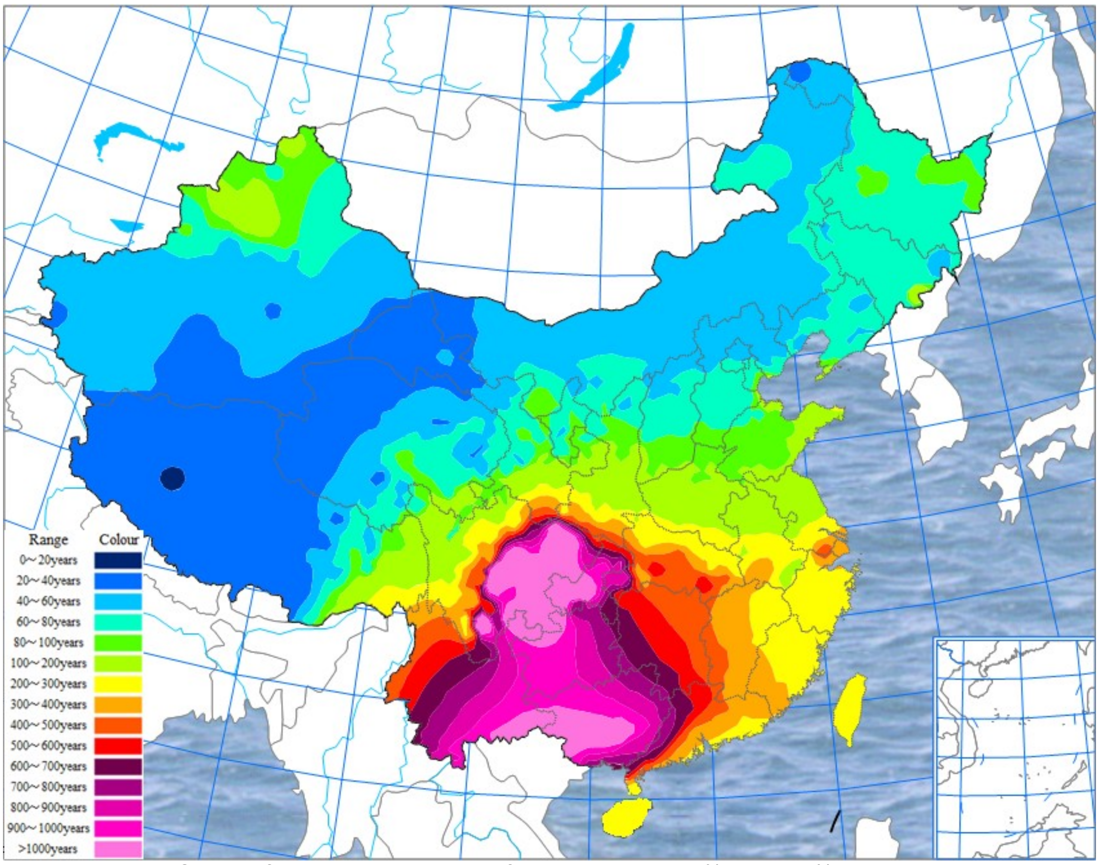

Fig.11 - Service life distribution map under freezing-thawing +10% load+5wt% sulphate solution

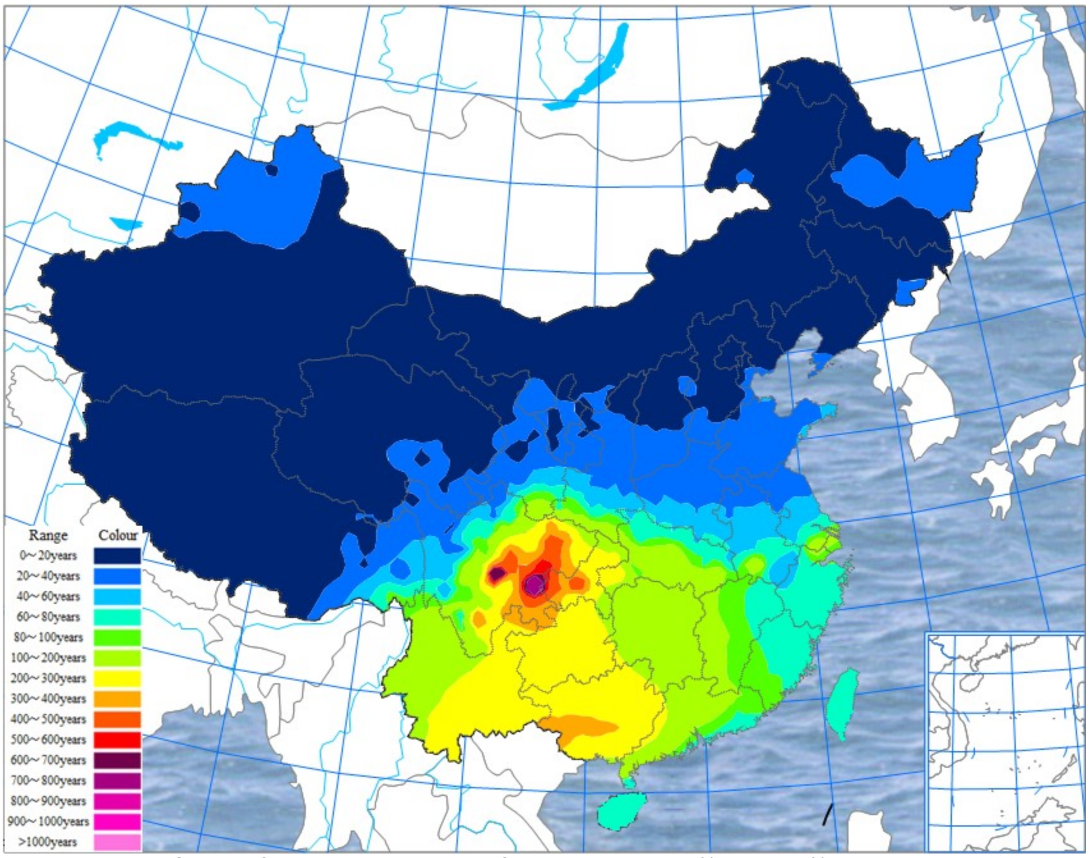

Fig.12 - Service life distribution map under freezing-thawing +30% load+5wt% sulphate solution

which accounted for 75% of the total 700 meteorological stations in the country, and the remaining 25% of the meteorological stations were located in South China, which was not threatened by freezing-thawing damage, therefore, they are not included, and the time span is from 1980 to 2013, which lasts for 34 years [23].

According to the freezing-thawing fatigue equation, the number of freezing-thawing cycles under water freezing, load and salt freezing environment is substituted into the equation and then combined with the indoor maximum temperature drop rate (take 11 °C/h), then according to the number of natural freezing-thawing cycles, the daily minimum temperature, the daily maximum temperature drop rate and other indicators, we can predict the national freezing-thawing life of the black bricks. Using GIS software TopMap7, we can draw various freezing-thawing life distribution maps of black bricks under water freezing, load and salt freezing environment. See Figures 8, 9, 10, 11 and 12.

5. Conclusions

In this paper, three durability failure factors of freezing-thawing cycle, sodium sulfate corrosion and external compressive stress were selected for the durability test of black bricks under single, double and multiple factors. The conclusions are as follows:

(1) Under the action of the single factor of freezing and thawing, the relative dynamic elastic modulus of the black bricks tends to increase slightly at first and then decrease. The relative dynamic elastic modulus of the black brick samples dropped to about 0.60 after 80 freezing-thawing cycles. After that, as the peeling of the corner parts of the samples is uneven, the ultrasonic sound velocity cannot be detected by the ultrasonic instrument.

(2) The load effect has obvious influence on the relative dynamic elastic modulus, and the load action accelerates the decline rate of the relative dynamic elastic modulus of the test piece under the action of freezing and thawing. After applying 10% load and 30% load, the relative dynamic elastic modulus decreased to less than 60% after 60 and 35 freezing-thawing cycles respectively, which reaches the failure criteria of the test piece.

(3) The coupling effect of load and sodium sulfate has a more significant effect on the decrease of its relative dynamic elastic modulus. Under the action of 10% load and 5% sodium sulphate solution, and 30% load and 5% sodium sulphate solution, the relative dynamic elastic modulus decreased to below 60% after 35 and 20 freezing-thawing cycles respectively, reaching the failure criteria of the test piece.

(4) Combining with the freezing-thawing fatigue damage equation model, through the number of indoor freezing-thawing cycles of the black bricks, and according to the natural freezing and thawing cycles, the daily minimum temperature, the daily maximum temperature drop rate and other indicators all around the country, this paper used the GIS software TopMap7 to draw various freezing-thawing life distribution maps of black bricks under water freezing, load and salt freezing environment.

Acknowledgments

This work was supported by the Doctoral Foundation of Shandong Natural Science Foundation (ZR2018BEE038), the National Natural Science Foundation of China (51678277, 51778269) and the National Key Research and Development Program of China (2017YFC0703100).

REFERENCES

1. C.L. Chu, Constructing a new domestic discourse: the modern home in architectural journals and mass-market texts in early twentieth-century China, Journal of Architecture, 2017, **22**(6), 1066.
2. Y. Ouyang, Application of Huizhou Architectural Style in Modern Houses. Civil, Structural and Environmental Engineering, 2014, **838**, 2883.
3. W. Zhou, Y.M. Wang, X.Z. Gao, W.L. Zhu, Q. Xu and S. Xu, Architecture, evolution history and controlling factors of the Baiyun submarine canyon system from the middle Miocene to Quaternary in the Pearl River Mouth Basin, northern South China Sea, Marine and Petroleum Geology, 2015, **67**, 389.
4. W. She, M.R. Jones, Y.S. Zhang and X. Shi, Potential Use of Foamed Mortar (FM) for Thermal Upgrading of Chinese Traditional Hui-Style Residences. International Journal of Architectural Heritage, 2015, **9**(7), 775.
5. Y.S. Wang and Y.P. Duan, A Study on the Classiication and Value of Ming Dynasty Paifang in China: A Case Study of Paifang in Jinxi County. Journal of Asian Architecture and Building Engineering, 2016, **15**(2), 147.
6. L. Hua, C.C. Chen, H. Fang and X.X. Wang, 3D documentation on Chinese Hakka Tulou and Internet-based virtual experience for cultural tourism: A case study of Yongding County, Fujian, Journal of Cultural Heritage, 2018, **29**, 173.
7. J. Liu, Component-driven pocedural modeling for ancient Chinese architecture of the Qing Dynasty, International Journal of Architectural Heritage, 2018, **12**(2), 280.
8. Y.J.Kim and S. Park, Tectonic Traditions in Ancient Chinese Architecture, and Their Development, Journal of Asian Architecture and Building Engineering, 2017, **16**(1), 31.
9. J.Liu and Z.K. Wu, Rule-Based Generation of Ancient Chinese Architecture from the Song Dynasty, Acm Journal on Computing and Cultural Heritage, 2016, **9**(2), 212.
10. D. Yu, Experimental study on anti-seismic property of inorganic polymer concrete short columns after high temperature, Annales de Chimie - Science des Matériaux, 2017, **41**(3-4), 225
11. T. Kubota, M.A. Zakaria, S. Abe and D.H.C. Toe, Thermal functions of internal courtyards in traditional Chinese shophouses in the hot-humid climate of Malaysia, Building and Environment, 2017, **112**, 115.
12. Y.M. Zhang, L.T. Jia, H. Mei, Q. Cui, P.G. Zhang and Z.M. Sun, Fabrication, microstructure and properties of bricks fired from lake sediment, cinder and sewage sludge, Construction and Building Materials, 2016, **121**, 154.
13. Y.J. Tang, Z.D. Shao and T.L. Xu, Pore Structure of Ancient Chinese Bricks under Environmental Vicissitudes, Ksce Journal of Civil Engineering, 2016, **20**(5), 1895.
14. G.Y. Li, X.Y. Xu, E. Chen, J. Fan and G.J. Xiong, Properties of cement-based bricks with oyster-shells ash, Journal of Cleaner Production, 2015, **91**, 279.
14. G.Y. Li, X.Y. Xu, E. Chen, J. Fan and G.J. Xiong, Properties of cement-based bricks with oyster-shells ash, Journal of Cleaner Production, 2015, 91, 279.

15. K.L. Lin, L.S. Huang, J.L. Shie, C.J. Cheng, C.H. Lee and T.C. Chang, Elucidating the effects of solar panel waste glass substitution on the physical and mechanical characteristics of clay bricks, Environmental Technology, 2013, 34(1), 15.
16. X.Z. Wang, W.Y. Gao, S. Yan, M.H. Niu and G.S. Liu, Incorporation of sand-based breathing bricks with foamed concrete and humidity control materials, Construction and Building Materials, 2018, **175**, 187.
17. D. Eliche-Quesada, J.A. Sandalio-Perez, S. Martinez-Martinez, L. Perez-Villarejo and P.J. Sanchez-Soto, Investigation of use of coal fly ash in eco-friendly construction materials: fired clay bricks and silica-calcareous non fired bricks, Ceramics International, 2018, **44**(4), 4400.
18. P.F. Ahmadi, A. Ardeshir, A.M. Ramezanianpour and H. Bayat, Characteristics of heat insulating clay bricks made from zeolite, waste steel slag and expanded perlite, Ceramics International, 2018, **44**(7), 7588.
19. C.H. Zhang, J.S. Qiu, X. Guan, P.J. Hou, W. Huang, Research on thermal performance of external thermal insulation composite concrete wall block, International Journal of Heat and Technology, 2018, **36**(1), 277.
20. K.Yan, PhD thesis, Freezing-thawing Durability of Carbonized Concretes Subjected to Multiple Damage Factors, Nanjing University of Aeronautics and Astronautics, China, 2007.
21. R. Tepfers and T. Kutti, Fatigue-Strength of Plain, Ordinary, and Lightweight Concrete, Journal of the American Concrete Institute, 1979, **76**(5), 635.
22. C.C. Ike, Exponential fourier integral transform method for stress analysis of boundary load on soil, Mathematical Modelling of Engineering Problems, 2018, **5**(1), 33.
23. H.J. Ma, PhD thesis, Zonation and Frost Resistance Parameter Design for Durability of Airport Pavement Concrete in Cold Region, Nanjing University of Aeronautics and Astronautics, China, 2015.

****

MANIFESTĂRI ȘTIINȚIFICE / SCIENTIFIC EVENTS

Ultra-High Temperature Ceramics: Materials for Extreme Environment Applications,
June 7-10, 2020, The Lodge at Snowbird, Snowbird, Utah, USA

Interest in high temperature ceramic phases has been growing in recent years, with significant ongoing research programmes in many countries across the world. This has occurred because the conditions in which materials are required to operate are becoming ever more challenging as operating temperatures and pressures are increasing in all areas of manufacture, energy generation, transport and environmental clean-up. Often extreme temperatures are combined with severe chemical environments and exposure to high energy and, in the nuclear industry, to ionizing radiation. The production and processing of next-generation materials capable of operating in these conditions is non-trivial, especially at the scale required in many of these applications. In some cases, totally new compositions, processing and joining strategies have to be developed. The need for long-term reliability in many components means that defects introduced during processing will need to be kept to an absolute minimum or defect-tolerant systems developed, e.g. via fiber reinforcement. Modelling techniques that link different length and time scales to define the materials chemistry, microstructure and processing strategy are key to speeding up the development of these next-generation materials. Further, they will not function in isolation but as part of a system. It is the behaviour of the latter that is crucial, so that interactions between different materials, the joining processes, the behaviour of the different parts under extreme conditions and how they can be made to work together, must be understood.

This conference is the fifth of a regular series of meetings held every two to three years. The vision for this workshop is to have 5 main topic areas:

- Processing (including all processing steps, scale up issues and novel approaches);
- Environmental response (including thermodynamic considerations, oxidation behaviour, etc);
- Characterization (including thermomechanical properties, subscale testing, etc);
- Modelling (at all levels, from atomistic to processing and property related); and
- Applications (including high-speed flight, propulsion, and energy related).

Contact
http://www.engconf.org/conferences/materials-science-including-nanotechnology/ultra-high-temperature-ceramics-materials-for-extreme-environment-applications/

****